CHARACTERIZATION OF A BRAKE LINING COMPOSITE BASED ON AIELE FRUIT CORES (CANARIUM SCHWEINFURTHII) AND PALM KERNEL FIBERS (ELAEIS GUINEENSIS) WITH A UREA-FORMALDEHYDE MATRIX

Ndapeu Dieunedort, Demze Nitidem Augustine, Sikame Tagne Nicodème R., Ganou Koungang Morino Bernard, Defo Narcisse, Njeugna Ebénezer

Abstract— The role of brake linings is to slow down and stop moving parts by dissipating their kinetic energy through friction. However, these linings must be efficient, have a certain lifespan and the debris resulting from their wear must not have a strong impact on the environment and human health. Asbestos, which is a material traditionally used for this purpose is harmful to health. Since then, we have been looking for an alternative solution in a context where the automotive industry is becoming increasingly demanding. It is to meet these needs that the present project proposed to characterize brake linings based on Canarium schweinfurthi aggregates and palm kernel mesocarp fibers with a urea-formaldehyde matrix. The mass fractions and sizes of the aggregates, as well as the mass fraction of the fibers were the main optimization variants. It was thus possible to obtain light linings with a density of less than 1212.48 kg.m-3, with a dynamic friction coefficient of between 0.56 and 0.81 and a low wear rate of around 1.67.

Index Terms— brake lining, friction coefficient, wear rate, canarium schweinfurthii; palm kernel mesocarp fibers

1. INTRODUCTION

Safety is a major issue in the development of current vehicles, car manufacturers to increase this safety, improve braking systems. Whatever the types of brakes, stopping a vehicle involves transforming the kinetic energy accumulated by the vehicle during its movement into calorific energy produced by the friction of a member secured to the chassis and the other secured of the running gear. For disc brakes, the element attached to the chassis is a friction material called a lining and the element attached to the running gear is called a brake disc. In the past, this filling was made asbestos. For health reasons and for the protection of the environment, linked to the environment and the health of populations, this material has been banned from the production of friction materials [1]. Since then, several studies have been carried out with a view to proposing new materials which can guarantee braking safety. Some brake linings are ceramic matrix or metal matrix for braking developing, when the temperature gradients are very high [2]. However, most of the brake linings that are currently available on the market are organic matrix, but their constitution and production methods are still the prerogative of the manufacturers. The objective of our study is to propose an additional solution of brake linings made from local plant by-products. This alternative will help to valorize these by-products abandoned for the most part in nature. In general, the components of brake linings can be classified into three main groups: reinforcing fibers, binders and fillers [3].

In Cameroon, palm oil production from industrial and village plantations can be estimated at 230,000 tonnes per year [4]. This allows the appreciation of large amount of fibers and palm kernel hulls found in nature after extracting palm oil. Next to it, the alder is a tree that produces edible black fruits called Canarium Schweinfurthii, which contains a hard core which is thrown away after consumption of the fruit. These above-mentioned sub-products pose environmental problems. These plants with a high food potential are subject to much research to increase their productivity to meet the demand[5]. In view of the potential potential that these by-products would overflow, is it possible to use them as filler and reinforcement in composites to be used as an additional solution for brake linings?

In operation, the linings undergo various stresses.

Therefore, they must have a good resistance, to wear, to thermal fatigue, to the compression generated during braking and to guarantee a stable coefficient of friction under different conditions and over time[6] . The coefficient of friction varies from 0.3 to 0.6 [7].]. In this work, we will determine the physical properties and mechanical properties such as density and porosity, limit compressive strength, coefficient of friction, wear rate and braking efficiency of the composites produced.

2. MATERIALS AND METHODS

2.1 MATERIALS

The sub-products from the plants used in this work all come from Cameroon. The shells and fibers of palm kernels of the tenera variety were collected in the southwest region. The canarium schweinfurthii (NCS) comes from the western region of Cameroon.
The toppings that are being considered are made up of canarium schweinfurthii (NCS) core granules reinforced with mesocarp fibers from the palm kernel shell mesocarp with a urea-formaldehyde matrix.

2.2 CONSTITUENT CONDITIONING

Fibers and canarium schweinfurthii cores are cleaned of oil residues and then washed, dried, crushed and graded. The oil residues are removed from the palm kernel fibers by immersing them in a solution of caustic soda, with 1kg of fibers in two liters of solution. The caustic soda solution is obtained by pouring the soda into water previously heated to 70°C, at a rate of 20g of NaOH per litre of water. Drying can be done at room temperature or in an oven at a temperature of about 80°C for 1 hour.
Oil residues are removed from the NCS simply by washing with water. Drying can be done in an oven at about 80°C for 2 hours, which also removes the seed contained in the core.
Grinding is done mechanically followed by sieving using a series of sieves to produce the three adopted sizes. Some authors propose the sizes of the aggregates ranging from 630 µm to 53µm [3], but in the present work we shall adapt the sizes of 0.500 mm and 0.200 mm .

2.3 COMPOSITION FORMULATION

The proposed brake lining is a composite consisting of NCS as a filler, palm kernel mesocarp fibers as a reinforcement and urea formaldehyde as a matrix.
In order to determine the optimum lining, we have developed several formulations by varying the size and mass fraction of the aggregates as well as the mass fraction of the fibers. Table 1 shows the different combinations adopted..

TABLE 1: TYPOLOGY OF THE DIFFERENT FORMULATIONS

Samples		UF10-50-0.2	UF10-50-0.5	UF10-40-0.5	UF5-65-0.2	UF5-50-0.2	UF5-50-0.5	UF5-55-0.2	UF5-40-0.5	UF5-40-0.2
Resin		Urea Formaldehyde								
Mass fraction of components (%)	Fibers	10	10	10	5	5	5	5	5	5
	NCS	50	50	40	50	50	55	55	40	40
CNS sizes (mm)		0.2	0.5	0.2	0.2	0.5	0.5	0.2	0.5	0.2

the coding of samples follows the rule below:

$$XY\ i-j-k \begin{cases} \boldsymbol{XY\ designates\ the\ resin} \\ \boldsymbol{i}\ is\ the\ mass\ fraction\ of\ the\ fibers\ es\ \%. \\ \boldsymbol{j}\ is\ the\ mass\ fraction\ of\ loads\ \%. \\ \boldsymbol{k}\ is\ the\ size\ of\ the\ loads\ in\ mm \end{cases}$$

2.1 COMPOSITE ELABORATION

Elaboration begins with the weighing of the different components, followed by the mixing and the introduction of the mixture into the mould. The moulding is done at an isotherm of 140±5°C under a pressure of 11 MPa. Figure 1 shows the elaboration process of the linings in question.

FIGURE 1: LINING ELABORATION PROCESS

2.4 BULK DENSITY

The bulk density of the elaborated linings was determined by the Archimedean thrust method. Paraffin was used to isolate the samples, and in each case the successive weighing of the sample before and after the paraffin was applied made it possible to deduce and subtract the mass of the paraffin used from the knowledge of the density of the paraffin. The apparent volume of the sample is obtained by removing the volume of displaced water. The measured mass of the sample noted m and its apparent volume noted V allow the

bulk density of the samples to be calculated using equation (1)

$$\rho = \frac{m}{V} \quad (1)$$

2.5 Determination of porosity

Porosity is defined as the ratio of the volume of voids to the apparent volume of the porous medium [8]. It can also be measured by a densification rate calculation[9]. A high porosity of the material indicates a low conductivity.

Porosity (%) = 1- Densification rate (%) (2)

Densification rate (%) = $\frac{\rho_m}{\frac{1}{100}\sum_1^3 X_i \rho_i}$ (3)

$$XY\ i-j-k \begin{cases} \boldsymbol{XY\ designates\ the\ resin} \\ \boldsymbol{i}\ is\ the\ mass\ fraction\ of\ the\ fibers\ es\ \%. \\ \boldsymbol{j}\ is\ the\ mass\ fraction\ of\ loads\ \%. \\ \boldsymbol{k}\ is\ the\ size\ of\ the\ loads\ in\ mm \end{cases}$$

Xi = mass percentage of each constituent forming the mixture,

ρi = absolute density of each constituent in the formulation, Table 2 gives the density values for the constituents used in Equation 3.

Table 2: Constituent Densities

Constituents	Canarium schweinfurthii core	Palm kernel mesocarp fibers	Urea formaldehyde resin
Density (kg.m-3)	1226	1268	1280
Source	[10]	[11]	[12]

2.6 Compression Test

The compression test was carried out according to NBN B15-220 standards. The specimens of dimensions 20x20x20 mm3 are subjected to a normal uniaxial compression load, which varies almost statically until cracks appear on the specimen. A hydraulic cylinder is used to apply the load measured indirectly by the deformation of ring 1 using the digital comparator at 1000th and converted into a force by means of the known ring stiffness. A second comparator measures the deformation of the specimen. This allows the stress-strain curve to be plotted until cracks appear on the test specimen. The ultimate load is used to calculate the limit stress, knowing the cross-section of the specimen. Figure 2 shows the kinematic diagram and picture of the compression/deflection test device and a dial gauge are required for this test.

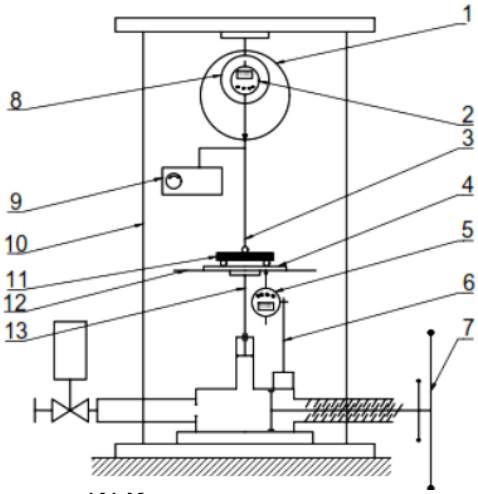

(A) Kinematic diagram

B) Picture

Figure 2 : *Compression-bending test machine*

2.7 Coefficient of friction measurement steel/lining and wear rate

2.7.1 Presentation of the disc-pin tribometer

The method adopted is that of dynamic friction of the pin-on-disc contact type. Figure 3 shows the kinematic scheme used. The black cast iron disc, held in the horizontal plane by a vertical transmission shaft, is set in motion by a three-phase electric motor through a pulley-belt system. The normal contact load is obtained by means of the marked masses which are placed in cage 4 linked on the one hand to the pin (consisting of the packing sample) and on the other hand to arm 11. The tangential dynamic friction force generated has the effect of bending arm 11. The measurement of the deflection of this arm makes it possible to calculate indirectly this tangential force noted FT. For a good reliability of the

tests, it is necessary to calibrate the tribometer arm before each campaign.

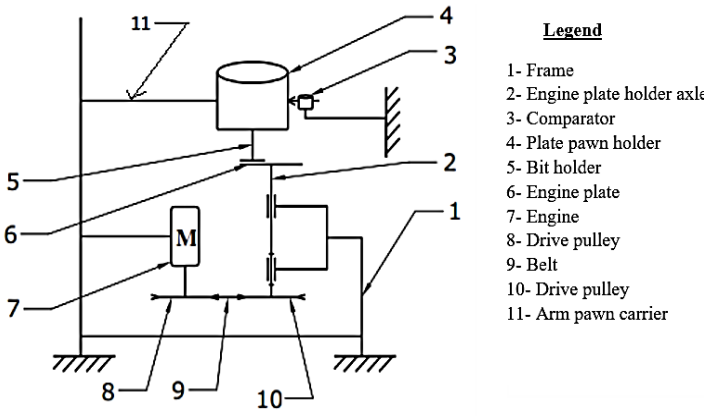

FIGURE 3: PAWN-DISC TRIBOMETER

2.7.2 TRIBOMETER CALIBRATION

Calibration of the tribometer consists of establishing the proportional relationship between the bending force and the deflection of the point of application of this force. Using a dynamometer, a force is imposed and a dial gauge at the 1000th is used to measure the relative deflection. By varying the imposed force noted F in the elastic range of the material, the corresponding deflections noted δ are obtained as shown in figure 4. This allows the force curve to be plotted as a function of the deflection called the calibration curve (figure 5). The slope of the linear regression line of the calibration curve (a=8.454) is the coefficient sought. Equation 6 gives the desired load-deflection relationship.

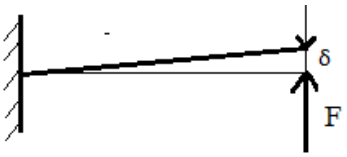

Figure 4: Schematic diagram of the calibration of the tribometer

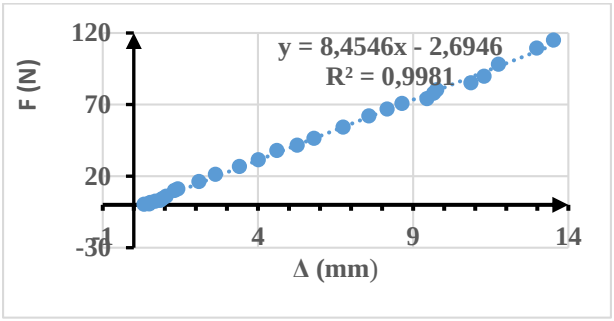

FIGURE 5: TRIBOMETER CALIBRATION CURVE

2.7.3 DETERMINATION OF THE FRICTION COEFFICIENT AND SPECIFIC WEAR

The disk pawn tribometer was used in dynamic friction tests. The pawn being the packing sample tested in prismatic form, while the disc is made of black cast iron. The normal contact load (FN=61.4N) is imposed by means of the centrifugal weights and the tangential friction force (FT) is measured indirectly by measuring the deflection of the peg arm. This deflection is converted into a force using the calibration coefficient. The dynamic coefficient of friction (μ) is calculated using equation 6 found in Sawyer's work disc-pawn tribometer was used in the dynamic friction tests. The pin being the lining sample tested in prismatic form, while the disc is made of black cast iron. The normal contact load (FN = 61.4N) is imposed using the counterweights and the tangential friction force (FT) is measured indirectly by measuring the deflection of the pin holder arm. This arrow is converted to force using the calibration coefficient. The dynamic coefficient of friction (μ) is calculated using equation 6 which is found in the works of Sawyer. [13]

$$\mu = \frac{F_T}{F_N} \quad (6)$$

The experimental conditions of dynamic friction in the present project, are gathered in Table 3.

TABLE 3: EXPERIMENTAL CONDITIONS FOR DYNAMIC FRICTION TESTS PIN ON DISC

Sizes	Normal Contact Load	Pawn-to-disk contact area	Contact radius	Sliding speed	Friction duration
Values	61,4 N	100 mm2	75 mm	10,8 m/s	5 min

The specific wear noted (W) is determined by measuring the mass of each sample before and at the end of each friction test. The mass loss due to wear noted Δm is used to calculate the specific wear from equation 8 from Rongping Yun's work..[14]

$$W = \frac{1}{d} * \frac{1}{F_T} * \frac{\Delta m}{\rho} \quad (8)$$

Where ρ is the bulk density of the lining sample and d is the friction distance and is calculated from the sliding velocity and friction time.

3. MEASUREMENT OF BRAKING EFFICIENCY

The MBT 2250 EUROSYSTEM brake tester, MCD 2000 version, was used to experimentally evaluate the braking efficiency of the different lining samples. The brake tester imposes a torque on both wheels of the same axle, uncoupled from the engine, of a conventional passenger car, whose total laden weight does not exceed 3.5 tonnes, on which the lining samples are mounted. The commercially

available (standard) lining is mounted on the front axle and the UF10-50-0.2 lining is mounted on the rear axle. When the braking system of the vehicle is activated, sensors at each wheel record the braking rate of each wheel. Braking efficiency is the sum of the braking forces on both wheels of a single axle divided by the total load of the axle in question. The load on the front wiper measured by the device is 924 DaN and on the rear axle is 700 DaN. In use, the limit values for unbalance between the right and left wheel of the same axle must be less than 30% at the front and 20% at the rear.

3.1 Bulk density and porosity of the different formulations

Table 3 shows the average bulk density values of the different packing samples. The UF5-40-0.5 formulation is the most dense and has the lowest porosity compared to the others as shown in the histogram in Figure 5.

Table 4: Summary of packing bulk densities and porosities

Samples	UF10-50-0.2	UF10-50-0.5	UF10-40-0.5	UF5-65-0.2	UF5-50-0.2	UF5-50-0.5	UF5-55-0.2	UF5-40-0.2	UF5-40-0.5
Porosity	4	11	3	8	4	4	5	9	1
bulk	1198.8	1108.2	1205.0	1157.0	1196.4	1198.4	1187.1	1146.9	1243.5

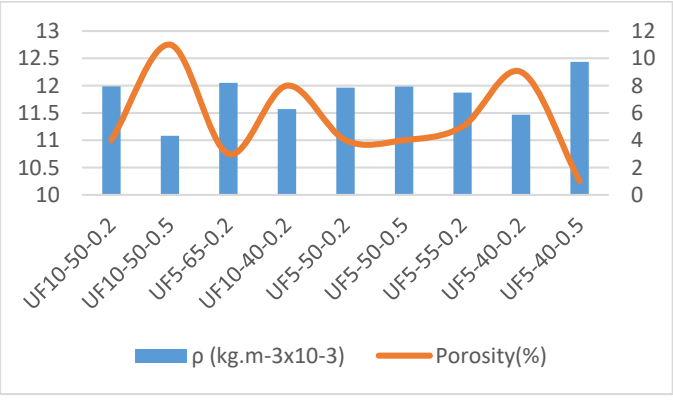

Figure 6: Density and Porosity Histogram

These bulk densities have been used in the calculation of the specific wear rate.

3.2 Dynamic friction coefficient

Figure 7 shows the overall pattern of the evolution of the dynamic coefficient of friction. It can be seen that this coefficient of friction remains stable for the first 150 seconds before experiencing a slight decrease.

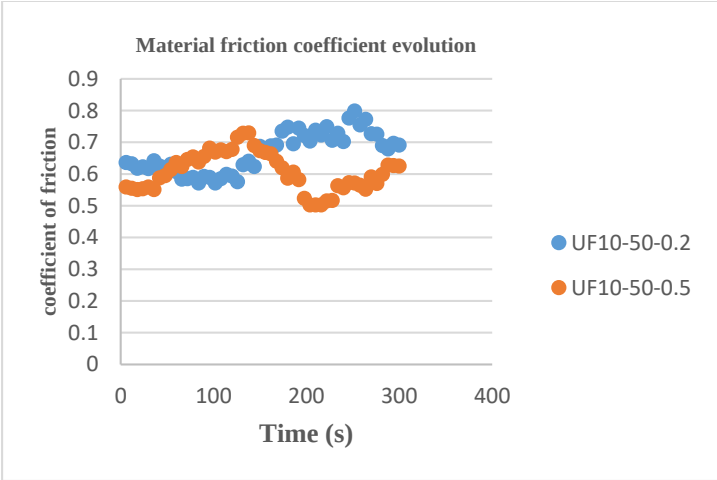

Figure 7 : Evolution course of the material friction coefficient

The The table summarizes the mean values of the coefficients of friction and the specific wear rates of all tested samples.

Table 5: Summary of friction coefficients

Samples	UF10-50-0.2	UF10-50-0.5	UF10-40-0.5	UF5-65-0.2	UF5-50-0.2	UF5-50-0.5	UF5-55-0.2	UF5-40-0.5	UF5-40-0.2
μ moy	0.70	0.52	0.38	0.55	0.44	0.43	0.43	0.64	0.67
Standard deviation	0.09	0.05	0.02	0.08	0.03	0.03	0.02	0.07	0.04
W(Cm3x10-7/Nm)	1,67	2,12	2,01	2,32	1,67	2,55	2,42	2,24	2,39
Standard deviation	0,76	5,5	0,65	0,85	0,54	0,76	0,8	0,3	0,59

The histogram in Figure 8 compares the values of the

coefficient of friction and the specific wear rate.

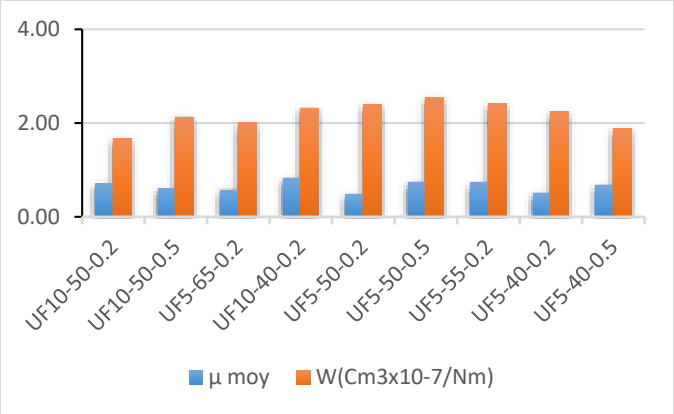

FIGURE 8: HISTOGRAM OF FRICTION COEFFICIENTS AND WEAR RATES

Good Good linings should have a high coefficient of friction and a low wear rate, therefore sample UF10-50-0.2 is selected for further testing. In addition, the wear rate of sample UF10-50-0.2 is among the best according to the work of Rongping Yun et al. in 2011[14], it places the best wear rates as those below 2.5 Cm3x10-7Nm..

3.3 LININGS COMPRESSION CHARACTERISTICS

3.3.1 RHEOLOGICAL BEHAVIOUR

Figures 9 show the stress-strain curve in uniaxial compression of the specimen UF10-50-0.2. The overall shape of this curve shows that it is a linear perfect elastic material. The slope of the linear regression line of normal compressive stress versus strain gives us Hooke's law Young's modulus in compression

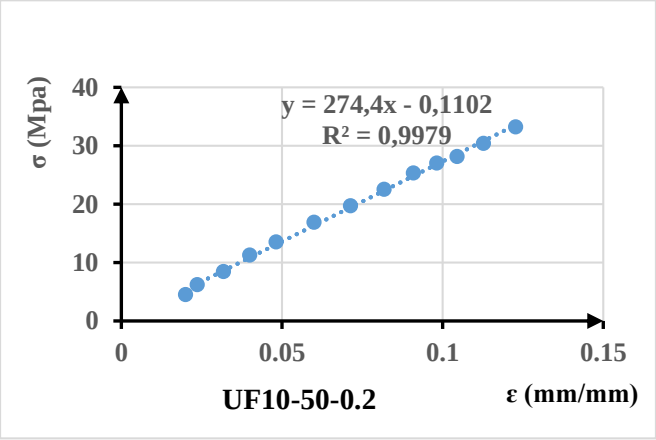

Figure 9: Curves Linings deformation constraint

3.3.2 YOUNG'S MODULUS IN COMPRESSION

Table 6 Table 6 shows the Young's modulus in compression of the UF10-50-0.2 formulation. The UF10-50-0.2 packing is stiffer in compression than the packing marketed according to [15] but on the other hand the latter is more tenacious

TABLE 6: *YOUNG'S MODULUS AND LIMITS LININGS CONSTRAINTS VALUES*

Material	Young's modulus (MPa)	Standard deviation	Limiting stress (MPa)	Standard deviation
UF10-50-0.2	**259,31**	**21,33**	**32,93**	**0,39**
Brake composite [15]	**150**	**-**	**30-50**	**-**

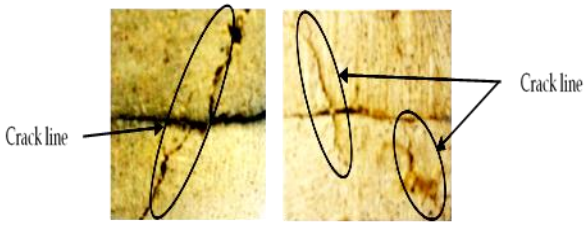

FIGURE 10: TEST SPECIMEN AFTER TESTING, LEFT THE M1 LINING AND RIGHT THE M2 LINING.

Braking pressures in a motor vehicle equipped with a disc and brake lining vary between 0.5 and 4 MPa. However, in extreme braking situations, the pressure can rise to 10 MPa [16]. It is noted that the developed linings can safely withstand high braking stresses except that at the limit compression, cracks appear on the surface of the linings (Figure 10).

3.3.3 BRAKING EFFICIENCY

The efficiency and percentage unbalance values recorded during efficiency testing of this packing are shown in Table 7. The unbalance of the front axle (standard) is 9% and the unbalance of the rear axle (UF10-50-0.2) is 5%. Both have a % imbalance of less than 30% front and 20% rear as recommended by the standard.

TABLE 7: BRAKING EFFICIENCY TEST RESULTS

Braking force in daN	% imbalance	Axle loading in daN	Braking efficiency
Model UF10-50-0.2 (rear axle)			

Left side	**Right side**			
215	**235**	**5%**	**700**	**64%**
Standard (front axle)				
237	**281**	**9%**	**924**	**56%**

Figure 11 shows the condition of the friction surfaces after testing, where a uniform wear can be seen at a glance on the commercially available (standard) lining as opposed to model UF10-50-0.2. This can be explained by the fact that the commercially available lining has a higher limit constraint.

A) B)

FIGURE 11 : FLOATING SURFACES OF LININGS AFTER PERFORMANCE TEST: A) UF10-50-0.2 LINING; B) COMMERCIALLY AVAILABLE LINING

3.3.4 SYNTHESIS AND COMPARISON OF RESULTS

Table 8 shows the comparison of the results with the existing one. Compared to commercial linings, the linings proposed in this project are less dense, stiffer, have a higher coefficient of friction and a low wear rate. All these characteristics remain within acceptable ranges compared to commercial brake linings.

TABLE 8: *COMPARISON OF THE RESULT WITH EXISTING FINDINGS*

	UF10-50-0.2	*Elephant grass*[17]	*palm kernel*	*Banana*	*Palm Kernel*	*Asbestos*[211]	*Commercial brake*
Bulk density ($kg.m^{-3}$)	*1198.8*	*1610*	-	-	-	*1320*	*1890*
Porosity(%)	*4*	*3.99-5.01*	-	-	*22.45*	*0.52-0.61*	-
Dynamic friction coefficient	*0.70*	-	*0.35*	*0.35*	*0.43*	-	*0,40*
Specific wear rate (Cm3x10-7/Nm)	*1,67*	*3.99*	*4.67*	*4.67*	*4.4*	*3.8*	*4,1*
Young's modulus (MPa)	*259,31*	-	-	-	-	-	*110*
Limit compression constraint (MPa)	*32,93*	*225-241*	*61.20*	-	*103*	*110*	*30-50*
Braking efficiency	*65%*	-	-	-	-	-	-

The Young's modulus in uni-axial compression of the linings developed by Lazim et al. [15] are close to the values of the linings in model UF10-50-0.2 of this project (see Table 3). The lining in this project is light, wears less, is stiffer and has better in-service braking efficiency than most linings in the literature, as shown in Table 5.

4- CONCLUSION

A brake lining based on Canarium schweinfurthi aggregates and palm nut mesocarp fibers with a urea-formaldehyde matrix was developed and characterized. By varying the mass percentage of the aggregates and fibres on the one hand and the size of the aggregates on the other hand, several formulations were developed in a well-established scientific protocol. Physical characteristics such as density and porosity; mechanical characteristics such as limiting constraint and uni-axial Young's modulus in compression; tribological characteristics such as dynamic coefficient of friction pawn on disc and specific wear rate identified the UF10-50-0.2 formulation as the best. In order for these to be recommended, additional tests on the long-term service life and thermo-hydro-tribological behaviour should be carried out.

REFERENCES

[1] P. Cattiau, G. Lasfargues, C. Barbieux, and A. Brizard, "Prévention du risque amiante dans les garages," *INRS*, vol. 69, no. 1er trimestre, pp. 37–43, 1997.

[2] J.-J. CARRÉ, "Technologie du freinage Organes de friction," *Tech. l'Ingénieur*, vol. 1, no. B5571, pp. 1–11, 1990.

[3] A.-L. Bulthé, "Caractérisation expérimentale du contact frottant disque garniture sous sollicitations sévères de freinage . Prise en compte des interactions tribologie , thermique et physico-chimie," 2007.

[4] A. Iyabano and L. Feintrenie, "Plantations villageaoises de palmier à huile et huile de palme artisanale au Cameroun," 2014.

[5] R. Njoukam and R. Peltier, "Article original Le gainage précoce des régimes de bananes améliore la croissance des fruits et leur état sanitaire vis-à-vis de l ' anthracnose (Colletotrichum musae)," *Fruits*, vol. 57, no. 2, pp. 239–248, 2002, doi: 10.1051/fruits.

[6] P. C. Verma, "Automotive Brake Materials : Characterization of Wear Products and Relevant Mechanisms at High Temperature," University of Trento, Italy, 2016.

[7] P. J. Blau, "Compositions , Functions , and Testing of Friction Brake Materials and Their Additives," 2001.

[8] M. Kacem, S. Salvador, and C. Jarlard, "Détermination expérimentale des propriétés structurales d ' un solide poreux hétérogène Introduction :," *Colloq. Fr. sur la Caractérisation Thermo-Physiques des Matériaux.*, pp. 1–7, 2003.

[9] N. Hentati, "Matériaux composites à matrice organique pour garnitures de frein : analyse des liens entre le procédé d ' élaboration , la microstructure , les propriétés et le comportement tribologique : analyse des liens entre le procédé d ' élaboration , la microstru," 2016.

[10] M. Ganou, D. Ndapeu, G. Tchemou, E. Njeugna, and L. Courard, "formulation des briques de terre bio sourcées à charge," in *4ème conférence scientifiques des doctorants et jeunes chercheurs des universités d'Etat / Instituts privés de l'enseignement supérieur*, 2019, pp. 1–4.

[11] P. W. H. Mejouyo *et al.*, "Physical and Mechanical Characterization of Several Varieties of Oil Palm Mesocarp Fibers Using Different Cross-Sectional Assumptions," *J. Nat. Fibers*, 2019, doi: 10.1080/15440478.2019.1612813.

[12] L. Gornet and H. Ijaz, "A high-cyclic elastic fatigue damage model for carbon fibre epoxy matrix laminates with different mode mixtures," *Compos. Part B Eng.*, 2011, doi: 10.1016/j.compositesb.2011.03.004.

[13] W. G. Sawyer, N. Argibay, D. L. Burris, and B. A. Krick, "Mechanistic Studies in Friction and Wear of Bulk Materials," *Annu. Rev. Mater. Res.*, vol. 44, pp. 395–427, 2014, doi: 10.1146/annurev-matsci-070813-113533.

[14] R. Yun, S. G. Martynková, and Y. Lu, "Performance and evaluation of nonasbestos organic brake friction composites with SiC particles as an abrasive," *J. Compos. Mater.*, vol. 45, no. 15, pp. 1585–1593, 2011, doi: 10.1177/0021998310385025.

[15] A. R. M. Lazim, M. Kchaou, M. K. A. Hamid, and A. R. A. Bakar, "Squealing characteristics of worn brake pads due to silica sand embedment into their friction layers," *Wear*, vol. 358–359, no. June, pp. 123–136, 2016, doi: 10.1016/j.wear.2016.04.006.

[16] M. Eriksson, F. Bergman, and S. Jacobson, "On the nature of tribological contact in automotive brakes," *Wear*, vol. 252, pp. 26–36, 2002, doi: 10.1016/S0043-1648(01)00849-3.

[17] N. O. Adekunle, K. A. Oladejo, R. Abu, K. T. Oriolowo, S. O. Ismaila, and S. M. Adegboyega, "Characterisation of Asbestos-Free Brake Pad Using Elephant Grass (Pennisetum Purpureum)," *Int. J. Sci. Eng. Res.*, vol. 11, no. 5, pp. 193–198, 2020.

[18] K. K. Ikpambese, D. T. Gundu, and L. T. Tuleun, "Evaluation of palm kernel fibers (PKFs) for production of asbestos-free automotive brake pads," *J. King Saud Univ. - Eng. Sci.*, vol. 28, no. 1, pp. 110–118, 2016, doi: 10.1016/j.jksues.2014.02.001.

[19] U. D. Idris and V. S. Aigbodion, "Eco-friendly asbestos free brake-pad : Using banana peels," pp. 185–192, 2015, doi: 10.1016/j.jksues.2013.06.006.

[20] A. O. A. Ibhadode and I. M. Dagwa, "Development of Asbestos-Free Friction Lining Material from Palm Kernel Shell," vol. XXX, no. 2, pp. 166–173, 2008.

[21] Z. U. Elakhame, O. A. Alhassan, and A. E. Samuel, "Development and Production of Brake Pads from Palm Kernel Shell Composites," vol. 5, no. 10, pp. 735–744, 2014.

[22] R. U. Rao and G. Babji, "A Review paper on alternate materials for Asbestos brake pads and its characterization," *Int. Res. J. Eng. Technol.*, vol. 2, no. 2, pp. 556–562, 2015.